ACS APPLIED BIO MATERIALS
Cite This: ACS Appl. Bio Mater. 2019, 2, 4966−4977
Article
www.acsabm.org

Colorimetric Detection of Mutant β-Amyloid(1−40) Membrane-Active Aggregation with Biosensing Vesicles

Michael P. Dorsey,[†,§] Brice M. Nguelifack,[‡] and Elizabeth A. Yates*[,†]

[†]Department of Chemistry, United States Naval Academy, 572M Holloway Road, Annapolis, Maryland 21402, United States
[‡]Department of Mathematics, United States Naval Academy, 572C Holloway Road, Annapolis, Maryland 21402, United States

Supporting Information

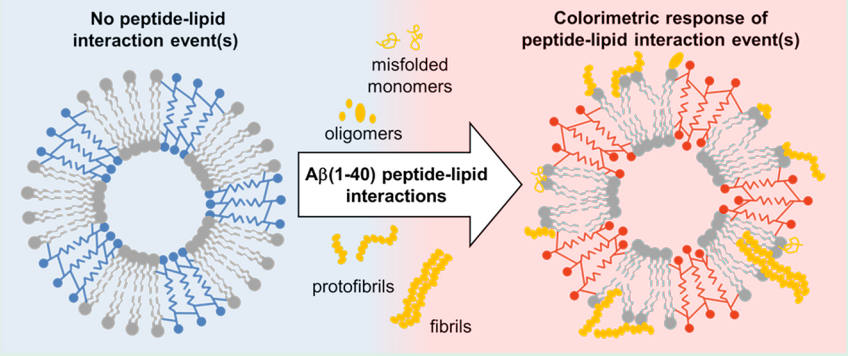

ABSTRACT: Alzheimer's disease (AD) is a protein misfolding disease commonly characterized by neuritic amyloid plaques and proteinaceous fibrillar aggregate deposits composed of β-amyloid (Aβ) aggregates. The dynamic aggregation of Aβ forms toxic, nanoscale aggregate species which proceed from oligomers to fibrils. Currently, there is need for rapid and direct detection of Aβ peptide aggregation and interaction with lipid membranes, as detecting an interaction with various lipid environments will provide insights to better understand how interactions may modulate membrane function on cellular surfaces, leading to the progression of AD. The goal of this study was to utilize a colorimetric, biomimetic, vesicle-binding assay as a biosensor to detect and investigate the occurrence of neurodegenerative disease-associated protein aggregation and interaction with lipid membranes. Lipid/polydiacetylene (PDA) vesicles were exposed to monomeric preparations of Wild Type Aβ(1−40) or point mutations in Aβ with amino acid substitutions that are commonly associated with familial AD (E22G Arctic, E22Q Dutch, A21G Flemish, D23N Iowa, and E22K Italian). We investigated how these substitutions affect Aβ(1−40) aggregation and interaction with lipid vesicles designed to mimic biological membranes. Time-resolved colorimetric measurements were obtained and reveal that exposure to lipid/PDA vesicle biosensors results in the direct detection of mutant Aβ(1−40) peptide−lipid interaction events. Aβ(1−40) peptide aggregate membrane activity varies among Aβ peptide variants and lipid composition. In addition, we used atomic force microscopy and Thioflavin T fluorescence assays to distinguish the stages of Aβ(1−40) aggregate formation, morphology, and membrane activity. These studies provide a simple means of aggregate detection and insight into the role of cellular surfaces in the mechanism of AD aggregation.

KEYWORDS: *aggregation, β-Amyloid peptide, colorimetric biosensor, polydiacetylene, membrane-active, peptide−lipid interactions*

INTRODUCTION

Protein folding is an essential function and fundamental example of biological self-assembly.[1] The amino acid sequence for natively folded proteins contains the information necessary to determine proper folding into a functional three-dimensional structure in a given environment.[2] The failure of proteins to fold correctly, or remain folded, causes a wide variety of pathological conditions, including neurodegenerative disease like Alzheimer's disease (AD).[1] Protein misfolding promotes the formation and deposition of self-assembled, highly ordered, toxic, insoluble, abnormal nanoscale β-sheet-rich proteinaceous fibrillar aggregates (commonly referred to as amyloids) within tissues or cellular compartments, resulting in damage to the cell and accompanying disease.[1,3−7] Globally, it is estimated that 34 million people suffer from AD alone, with numbers expected to triple by 2050.[8] Due to the ever-increasing number of people afflicted with neurodegenerative disease, the study of the physiological basis behind diseases associated with the rearrangement of specific proteins to non-native conformations is warranted.

Significant conformational changes can be induced in proteins encountering surfaces, and the interaction between amyloid-β (Aβ) and cellular surfaces is known to be important for disease toxicity.[9,10] Protein−surface interactions play a

Received: July 30, 2019
Accepted: October 21, 2019
Published: October 21, 2019

DOI: 10.1021/acsabm.9b00694
ACS Appl. Bio Mater. 2019, 2, 4966−4977

critical role in nucleating aggregate formation or stabilizing specific aggregation states with potential implications for protein-misfolding diseases. Surfaces of particular interest in such diseases are cellular and subcellular membranes. Studies have shown that changes in lipid membrane properties may induce amyloid aggregation and influence amyloid-damaging effects to a lipid cellular membrane.[11−15] Due to the dynamic aggregation mechanism of amyloidogenic proteins (i.e., misfolded monomers to globular oligomeric precursors to mature fibrils), techniques capable of rapidly detecting membrane-active aggregate species and their surface interaction events within a heterogeneous aggregation reaction are needed.

Research shows that lipid vesicle/polydiacetylene (PDA) matrices provide a model system to mimic cellular membrane composition with high reproducibility and stability.[16−18] These biosensors are composed of diacetylene monomers of 10,12-tricosadiynoic acid (TRCDA). An important feature of TRCDA polydiacetylenes are their colorimetric properties. In the presence of lipids, these species self-assemble and incorporate lipids into the PDA matrix to form an integrated colorimetric, biomimetic vesicle. The lipid/PDA vesicle formed has an overall blue appearance once irradiated in aqueous environments.[19−21] Lipid components in the vesicle form distinct domains with biosensing abilities. The yielded vesicle-based colorimetric biosensor undergoes visible blue-to-red color transitions in the presence of environmental perturbations such as Aβ peptide activity (i.e., aggregation and interaction) with a lipid domain, interfacial pressure, and pH changes.[20,22−25] In this study, we hypothesize that membrane-active Aβ(1−40) peptide aggregation (in association with vesicle−peptide interactions) is affected by changes in lipid surface chemistries. In addition, we aimed to demonstrate the use of colorimetric vesicle-binding assays as a valid biosensor to aid in the direct detection of vesicle−peptide aggregation and interaction events associated with AD. To identify and detect the role of amyloid protein surface interaction in the presence of various lipid chemistries, we studied three lipid vesicle systems with polydiacetylene (PDA) to form lipid/PDA biosensors: (1) total brain lipid extract (TBLE), (2) 1,2-dimyristoyl-*sn*-glycero-3-phosphocholine (DMPC), and (3) 1,2-dimyristoyl-*sn*-glycero-3-phospho-(1′-rac-glycerol) (DMPG). These lipid systems have been found to form lipid-functionalized PDA vesicles for many applications (i.e., detection of receptor−ligand interactions, antimicrobial peptides, amyloidogenic peptide sequences, food borne bacteria, and pathogens) and were selected to be studied with amyloidogenic proteins.[17,21,25−28] TBLE bilayers contain a physiologically relevant mix of lipid components (i.e., cholesterol, gangliosides, sphingolipids, isoprenoids, and both acidic and neutral phospholipids); DMPC is a neutral phospholipid, and DMPG is an anionic phospholipid (Figure S1).

We hypothesize lipid/PDA systems to serve as an appropriate model lipid surface for our investigation to detect lipid surface interaction events and membrane activity induced by amyloidogenic Aβ(1−40) peptide aggregation. We compare Wild Type Aβ(1−40) and five different Aβ(1−40) peptides associated with familial AD (FAD), Arctic (E22G), Dutch (E22Q), Flemish (A21G), Iowa (D23N), and Italian (E22K) (Figure 1) to investigate how amino acid substitutions affect aggregation states and interactions with a lipid membrane surface. These point mutations have been shown to alter the

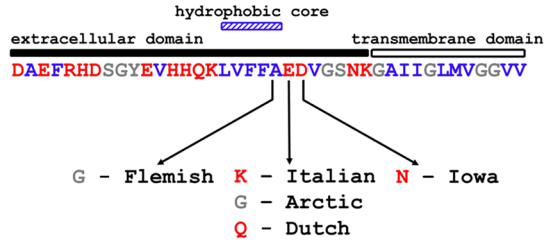

Figure 1. Schematic representation of Aβ(1−40) sequence (Wild Type), and five familial point mutations occurring at positions 21−23 used in this study (i.e., Arctic, Dutch, Flemish, Iowa, and Italian). Each amino acid is labeled hydrophobic (blue), hydrophilic (red), and slightly hydrophobic (gray) using the hydropathy index.

rate of Aβ aggregation[29−35] and have a propensity to form heterogeneous mixtures of aggregate states and polymorphic aggregates in the presence of lipid bilayers.[11,36,37] In addition, the hydrophobic[38] and electrostatic properties of Aβ peptide mutations may play a key role in affecting its ability to interact, insert, and potentially disrupt the structural integrity of bilayers in a mutation-dependent manner over time.[11] Such variations are due to the change in charge from an amino acid substitution of the Aβ(1−40) peptide which greatly affects aggregation state morphology and kinetics, and results in differing lipid membrane surface interactions. Previous simulation studies have indicated an increase in amyloid formation (*in vitro*) for the Arctic mutation and drastically reduced for the Flemish mutation (in comparison to Wild Type), while coarse-grained protein models have found the Flemish mutation to strongly favor the monomeric peptide and Arctic to favor protofibrils/fibrils.[29,39]

We suspect varied membrane-active peptide aggregation and peptide−lipid interaction at 44 h, based on both the aggregation state and mutant peptide surface chemistry (i.e., Arctic, Italian, Iowa, and Wild Type Aβ(1−40) to be mostly in the protofibril/fibril state with some oligomers present, Dutch and Flemish to be in the oligomer/protofibril state). Knowing key aggregation details of point mutations in the hydrophobic central region of Aβ(1−40), we sought an easier and more straightforward way to investigate and detect membrane-active Aβ peptide aggregation with simple, model membranes. Here, we use a vesicle-binding assay to monitor Aβ aggregation that will occur exclusively at the lipid bilayer inducing a detectable, visible colorimetric transition. In addition, to determine the most membrane-active Aβ(1−40) aggregation states, we utilized biophysical characterization via *ex situ* AFM and Thioflavin T (ThT) fluorescence assays. The current work provides the framework for utilizing the lipid/PDA vesicle biosensor system as a means to mimic cellular membranes and measure amyloidogenic peptide−membrane interaction events in real time. We report a new use of a colorimetric, biomimetic, vesicle-binding assay to serve as a biosensor for neurodegenerative protein interaction with lipid membranes.

METHODS AND MATERIALS

Materials. Synthetic, lyophilized Wild Type (WT), Arctic, Dutch, Flemish, Iowa, and Italian Aβ(1−40) peptides were acquired from AnaSpec Inc. (San Jose, CA). Total brain lipid extract (TBLE) (porcine), 1,2-dimyristoyl-*sn*-glycero-3-phosphocholine (DMPC), and 1,2-dimyristoyl-*sn*-glycero-3-phospho-(1′-rac-glycerol) (sodium salt) (DMPG) were purchased from Avanti Polar Lipids (Alabaster, AL). Diacetylene monomers of 10,12-tricosadiynoic acid (TRCDA) were purchased from GFS Chemicals (Powell, OH). Bovine serum

DOI: 10.1021/acsabm.9b00694
ACS Appl. Bio Mater. 2019, 2, 4966−4977

albumin (BSA), 1× Tris-buffered saline (TBS), hexafluoroisopropanol (HFIP), dimethyl sulfoxide (DMSO), sodium hydroxide (NaOH), and Thioflavin T (ThT) (ACROS Organics) were purchased from Thermo-Fisher Scientific (Hanover Park, IL). For AFM imaging, muscovite mica (Grade V5) was purchased from Ted Pella (Redding, CA), and ScanAsyst-Air AFM probes were purchased from Bruker (Santa Barbara, CA).

Preparation of Lipid/PDA Vesicles. The lipid/PDA vesicle systems composed of various lipids (TBLE, DMPC, or DMPG) were prepared using previously reported protocols.[16,22,23] In summary, vesicles containing the corresponding lipid (TBLE, DMPC, or DMPG) and diacetylene monomers of TRCDA (2:3 molar ratio) were dissolved in a 1:1 chloroform/ethanol solution and volatiles removed under reduced pressure, leaving behind a thin, dry solid film. Hot 1× TBS (≥70 °C), pH 7.4, was added to each dried lipid/PDA sample, and samples were sonicated for 5 min. To promote self-assembly of the vesicles, each vesicle suspension was cooled to room temperature, sealed, covered in aluminum foil, and stored at 4 °C for 24 h. The lipid vesicles and colorless diacetylene monomers of TRCDA were polymerized at room temperature following UV irradiation at 254 nm with 7 lm for 10−15 min with stirring, as indicated by a color change to blue. The lipid/PDA vesicle suspension was stored at 4 °C and was stable for up to 6 months.

Preparation of Aβ(1−40) Peptides. Synthetic, lyophilized Wild Type, Arctic, Dutch, Flemish, Iowa, and Italian Aβ(1−40) peptides were prepared as reported previously.[24] Briefly, Aβ(1−40) peptides were treated with HFIP to dissolve any preexisting aggregates and/or seeds present in the lyophilized stocks. HFIP was removed completely under reduced pressure, and thin peptide films were recovered. Each Aβ(1−40) peptide film was dissolved in DMSO to make a 2.5 mM stock solution. The initial peptide concentration of each Aβ(1−40) stock was measured using the Protein A280 assay of a NanoDrop 2000C spectrophotometer (Thermo Scientific), and a final peptide concentration of ∼20 μM was prepared in 1× TBS, pH 7.4, at 37 °C. All peptide stock solutions of Wild Type Aβ(1−40) and mutant Aβ(1−40) were flash frozen and stored at −20 °C to prevent inducing additional aggregation at higher temperatures.

Lipid/PDA Colorimetric Vesicle Assay. All lipid/PDA vesicles were warmed to room temperature with gentle stirring prior to each assay. Each peptide stock solution was thawed at 37 °C and sonicated for 20 min at 25 °C to disrupt any aggregates formed. Peptide/vesicle interactions were measured in 1× TBS, pH 7.4, containing polymerized lipid/PDA and ∼20 μM of each peptide. Each experiment was performed in triplicate in a 96-well plate (clear, nontreated, polystyrene), at wavelengths of 630 and 490 nm over the course of 44 h with with a SpectraMax M5 microplate reader (Molecular Devices) at 25 °C. Measurements of only lipid/PDA in 1× TBS (without the addition of protein) and 20 μM BSA prepared in 1× TBS were carried out for each biosensor to serve as the controls. The results were verified among three or more independent experiments. Quantitatively, the value for the blue-to-red color transition is given by the percent colorimetric response (% CR):

$$\%\ \text{colorimetric response} = \left[\frac{(\text{PB}_0 - \text{PB}_1)}{\text{PB}_0}\right] \times 100\%$$

where

$$\text{PB} = \frac{A_{\text{blue}}}{(A_{\text{blue}} + A_{\text{red}})}$$

Of note, "blue" (630 nm) and "red" (490 nm) refer to the visual appearance of the lipid/PDA vesicle. PB_0 is the red/blue ratio of the initial control sample (blue vesicles) before the initiation of a color change. PB_1 is the final value obtained for the lipid/PDA assay after the addition of peptides. All % CR values were averaged over 3−4 samples.

Aβ(1−40) Aggregation and Ultracentrifugation. All peptide stocks (2.5 mM) were prepared in DMSO. Stocks were diluted to 20 μM in 1× TBS buffer, pH 7.4. In order to generate aggregates, peptide solutions were incubated at 37 °C and 300 rpm for 44 h. To separate the supernatant and aggregates, solutions were centrifuged at 45 000 rpm for 1 h at 4 °C in a Sorvall WX Ultra Series centrifuge (Thermo Scientific). The supernatant was transferred to another Eppendorf tube, while pellet fractions were resuspended in 0.5 mL of 1× TBS.

Thioflavin T (ThT) Fluorescence Aggregation Assays. Aβ peptides (∼20 μM) were incubated in 100 μM ThT (10 μL) in 1× TBS, pH 7.4 (without lipid/PDA vesicles), or in 100 μM ThT (10 μL) in 1× TBS, pH 7.4, containing polymerized lipid/PDA (with lipid/PDA vesicles: TBLE/PDA, DMPC/PDA, and DMPG/PDA). All assays were done in a 96-well plate (black with clear bottom, nontreated, polystyrene) and sealed to prevent evaporation. Samples were excited at 440 nm, and ThT fluorescence emission was detected at 480 nm at 25 °C on a SpectraMax M5 microplate reader (Molecular Devices). For time course assays, fluorescence was measured every 15−30 min with 2 s shaking between reads for up to 160 h. Representative ThT aggregation curves provided kinetic data that was fitted with a sigmoidal model[40] to estimate T_{lag} (lag time) and $T_{1/2}$ (time at half completion of the aggregation process). All ThT assays were performed in triplicate and results verified among independent experiments. ThT assay results were plotted in arbitrary units (a.u.).

Lipid/PDA Colorimetric and Thioflavin T Assays with Aggregated Aβ(1−40) Fractions. For additional membrane interaction assays, % CR was measured after adding each 44 h, ultracentrifuged, aggregated fraction (supernatant or pellet) to each lipid/PDA vesicle. % CR was measured in 1× TBS, pH 7.4, containing polymerized lipid/PDA and ∼20 μM of each aggregated peptide. Each experiment was performed in triplicate in a 96-well plate (clear, nontreated, polystyrene), at wavelengths of 630 and 490 nm over the course of 44 h with a SpectraMax M5 microplate reader (Molecular Devices) at 25 °C. Fraction concentrations were verified using the Protein A280 assay of a NanoDrop 2000C spectrophotometer (Thermo Scientific). In addition, aggregated fractions were incubated with ThT (for 2 h), and the maximum fluorescences of two or more individual samples were averaged and reported with standard error. Pure lipid/PDA vesicles were added to each well, and fluorescence measurements were collected for 2 h. All ThT assays were performed in triplicate and results verified among independent experiments.

***Ex Situ* Atomic Force Microscopy (AFM) Imaging Conditions.** For experiments to study the aggregation of Aβ(1−40) peptides added to the lipid/PDA biosensors under *ex situ* conditions, 20 μM solutions of each peptide were prepared in 1× TBS and incubated at 37 °C and 300 rpm. Time points were taken at 0, 1, 8, 12, 24, and 44 h by diluting each Aβ(1−40) peptide into 1× TBS, and 5 μL aliquots of each incubation were spotted on freshly cleaved mica. Samples were allowed to dry, subsequently washed with 250−500 μL of HPLC grade water, and further dried under a gentle stream of nitrogen. Three samples of each Aβ(1−40) peptide were prepared and sampled twice at each time point.

For experiments to characterize the obtained lipid/PDA vesicles in terms of size, dispersity, and lamellarity under *ex situ* conditions, 5−10 μL samples of each polymerized lipid/PDA solution were spotted on freshly cleaved mica, allowed to dry, washed with 250−500 μL of HPLC grade water, and further dried under a gentle stream of nitrogen. Three different lipid/PDA assay solutions were made and characterized for each lipid/PDA vesicle composition. Each vesicle solution was sampled twice. Aβ(1−40) peptide aggregates and lipid/PDA vesicles deposited on mica were imaged *ex situ* via a Nanoscope V MultiMode 8 scanning probe microscope (Bruker, Santa Barbara, CA) equipped with a closed-loop vertical engage J-scanner and operated in the ScanAsyst-Air mode (a PeakForce tapping mode, Bruker). Images were taken with a ScanAsyst-Air silicon nitride cantilever of triangular geometry with a nominal spring constant of 0.4 N/m, a nominal tip radius of 2 nm, and a nominal resonant frequency of 70 kHz. Scan rates were set at 1−2 Hz. ScanAsyst mode continuously monitors image quality and makes automatic appropriate image parameter adjustments.

Quantitative Image Analysis. AFM image processing was completed using Gwyddion 2.50 free software[41] (Czech Metrology Institute). To determine size of lipid/PDA vesicles, particle analysis

DOI: 10.1021/acsabm.9b00694
ACS Appl. Bio Mater. 2019, 2, 4966−4977

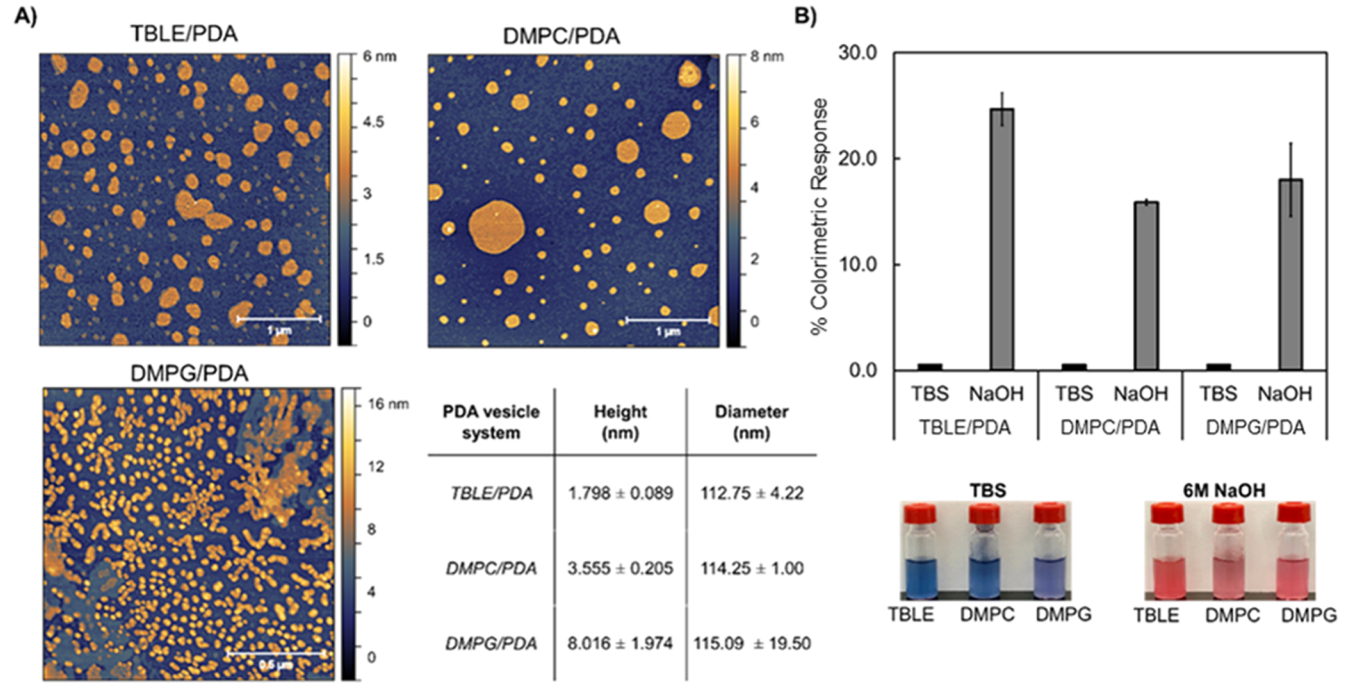

PDA vesicle system	Height (nm)	Diameter (nm)
TBLE/PDA	1.798 ± 0.089	112.75 ± 4.22
DMPC/PDA	3.555 ± 0.205	114.25 ± 1.00
DMPG/PDA	8.016 ± 1.974	115.09 ± 19.50

Figure 2. Lipid/polydiacetylene biosensor formation and response. (A) Representative *ex situ* AFM images of TBLE/PDA, DMPC/PDA, and DMPG/PDA after vesicle formation and polymerization with height and diameter. (B) Lipid/PDA vesicles are stable through 44 h of exposure to 1× TBS (pH 7.4) and NaOH solution (6 M, pH 12). Error bars represent standard deviation. Upon exposure to 1× TBS, lipid/PDA vesicles stay blue in color, while exposure to 6 M NaOH results in lipid/PDA vesicles turning pink/red.

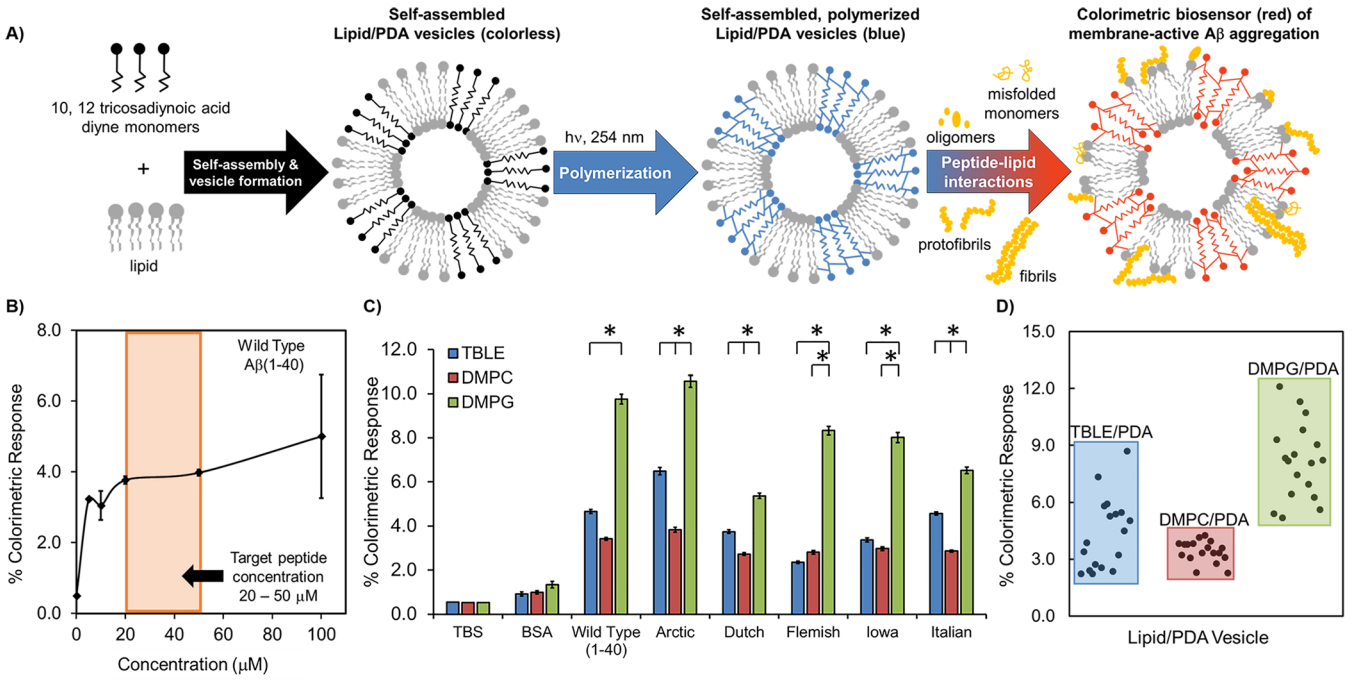

Figure 3. Percent colorimetric response (% CR) of lipid/PDA vesicles exposed to Aβ(1−40) peptides as a function of time. (A) Schematic illustration of lipid/PDA vesicle biosensor self-assembly, polymerization, and color change in response to peptide−lipid interactions or environmental perturbations. (B) Representative dose response curve of Wild Type Aβ(1−40). The dose response curve shows a plateau in % CR from concentrations of 20−50 μM (the targeted Aβ(1−40) peptide concentration region). (C) The overall average % CR at 44 h is shown for TBS, BSA, and each lipid/PDA vesicle with standard error. A comparison of % CR differences between each Aβ(1−40) peptide and the three lipid/PDA vesicle systems was performed via ANOVA and Tukey post hoc tests. (D) % CR obtained for all lipid/PDA vesicle experiments with Wild Type, Arctic, Dutch, Flemish, Iowa, and Italian Aβ(1−40) peptides.

was performed on multiple *ex situ* AFM images using supplier-provided software NanoScope v9.0 for MultiMode 8 SPM (Bruker, Santa Barbara, CA) with detection threshold heights of 2−8 nm, total count of 100−300 particles. The height histogram analysis was done using Gwyddion 2.50.

DOI: 10.1021/acsabm.9b00694
ACS Appl. Bio Mater. 2019, 2, 4966−4977

Statistical Analysis. Tukey post hoc tests were used to investigate the pairwise difference between lipids. For statistical analysis, a prior investigation (i.e., normality of two samples for the two sample *t*-test and/or ANOVA) was conducted on the data to ensure adequacy and accuracy. ANOVA was performed to investigate the significant difference for each Aβ(1−40) peptide among the different lipid/PDA biosensors. Most analyses were performed using the statistical software R version 3.1.0 or higher. All analyses and graphs were obtained from statistical software RStudio version 1.1.383 using the statistical package "ggplot2" (GNU project operating system, The R foundation).

RESULTS

Lipid/PDA Biosensor Formation and Response. To verify proper lipid/PDA vesicle formation, we characterized all three lipid/PDA vesicle-based biosensors in terms of size, dispersity, and lamellarity under *ex situ* conditions using AFM (see the Methods and Materials section). The model biological lipid systems investigated are composed of varying components: total brain lipid extract (TBLE), 1,2-dimyristoyl-*sn*-glycero-3-phosphocholine (DMPC), and 1,2-dimyristoyl-*sn*-glycero-3-phospho-(1′-rac-glycerol) (DMPG) (Figure S1). All lipid/PDA vesicles appear as large, unilamellar vesicles (LUVs), which are defined as small circles being full, with no stacking of bilayers visible (Figure 2A),[42] and the polydispersed lipid/PDA vesicle systems are shown to have varied parameters based on lipid composition (Figure 2A). By characterizing lipid/PDA biosensors in terms of size, dispersity, and lamellarity, we are able to use lipid/PDA vesicles as a vesicle-based colorimetric sensor system to measure the interaction of a biological analyte, Aβ(1−40) peptides, and lipid interfaces of varied compositions.

Environmental changes induced by the interaction event give rise to a blue-to-red color shift of the PDA polymer (Figure S2). This colorimetric response is due to changes in the TRCDA polymer backbone. Quantitatively, the value of the blue-to-red transition is given by the percent colorimetric response (% CR). To test the response of each lipid/PDA vesicle biosensor, we exposed the biosensor systems to 1× TBS (negative control) or 6 M NaOH (positive control). NaOH promotes lipid decomposition by changing the tension in the vesicle, inducing a high colorimetric response. For all three lipid/PDA vesicle-based biosensors, exposure to NaOH resulted in a positive and enhanced % CR over a 44 h period (Figure 2B). Thus, this data indicates that our lipid/PDA vesicle biosensor systems produce a colorimetric response in response to external perturbations.[23]

Aβ(1−40) Peptide−Surface Interactions Can Be Detected by Lipid/PDA Biosensors. Using the lipid/PDA biosensor, we tested our hypothesis that changes in lipid composition alter physical properties of lipid membranes, modulate peptide aggregation associated with neurodegenerative FAD, and promote vesicle−peptide molecular interactions. In the assay, lipid components in the self-assembled, polymerized lipid/PDA vesicles form distinct bilayer domains with biosensing abilities. When associated with Aβ(1−40) peptides, lipid/PDA vesicle biosensors can sense surface interactions and aggregation via a rapid colorimetric transition (blue to red) (Figure 3A). The analysis of the colorimetric, biosensing vesicle assay illustrates how Aβ(1−40) peptides both aggregate and interact with model lipid domains in solution. A representative dose response curve for Wild Type Aβ(1−40) shows a plateau in % CR in our targeted peptide concentration region of 20−50 μM (see Figure 3B). All peptides studied are Aβ variants with single amino acid substitutions of Wild Type Aβ(1−40); therefore, experiments were completed at the same concentration within this range. Aβ(1−40) peptides studied were evaluated for their ability to elicit a % CR at ∼20 μM. 20 μM has been shown to be the most neurotoxic concentration of $A\beta_{1-42}$ and a widely used physiological concentration for $A\beta_{1-40}$ and $A\beta_{1-42}$ studies.[26,43,44] We attribute differences in % CR curves among peptides to be consistent with membrane-active aggregation states present. To measure the peptide−lipid interaction via perturbation of the lipid bilayer surface by membrane-active aggregate states, we exposed each Aβ(1−40) peptide to several model lipid/PDA vesicle compositions including TBLE/PDA, DMPC/PDA, and DMPG/PDA. All Aβ(1−40) peptides (Wild Type, Arctic, Dutch, Flemish, Iowa, and Italian) promoted a colorimetric response with each lipid/PDA vesicle over a 44 h period (Figure 3C,D). DMPG/PDA vesicles consistently produced the highest colorimetric response among all Aβ(1−40) peptide experiments (n = 56 experiments, average % CR 5.365−10.571%), followed by TBLE/PDA (average % CR 2.358−6.480%), and DMPC/PDA (2.731−3.836%) (Figure 3D).

In all lipid/PDA assays, the Arctic peptide elicited the largest colorimetric response of all Aβ(1−40) peptides (Figure 3C). Wild Type peptide also interacts strongly with the lipid/PDA vesicles identified here, albeit less effectively than Arctic. The remaining peptides display distinct variability in the elicited colorimetric response (Figure 3C). We used statistical analysis software to analyze the differences between lipid/PDA pairs (i.e., TBLE/PDA-DMPC/PDA, TBLE/PDA-DMPG/PDA, and DMPC/PDA-DMPG/PDA) correlating to a varying degree of % CR with each vesicle-to-Aβ(1−40) peptide interaction. Quantitative analysis determined that significant differences in % CR were present among the lipid/PDA biosensor systems in association with each individual vesicle−peptide interaction (* indicates $p < 0.0005$) (Figure 3C, Figure S3). All Aβ(1−40) peptides in this study demonstrate a significantly higher interaction overall with the DMPG/PDA vesicle system. Statistical analysis suggests that the average % CR values of both TBLE/PDA and DMPC/PDA vesicles were significantly lower than those for DMPG/PDA vesicles for Wild Type Aβ(1−40) and each Aβ (1−40) peptide variant. In addition, Wild Type, Arctic (E22G), Dutch (E22Q), and Italian (E22K) Aβ(1−40) peptides show that an average % CR of TBLE/PDA was significantly higher than that of DMPC/PDA. It is important to note that these three point mutations, which have the most unique interactions with the varied lipid compositions of vesicles, occur at the same amino acid (Arctic (E22G), Dutch (E22Q), and Italian (E22K)). These statistical comparisons demonstrate the effect of aggregation state formed by each Aβ(1−40) peptide on each vesicle−peptide interaction and support our hypothesis in demonstrating how lipid composition modifies peptide aggregation and stimulates differences in vesicle−peptide interactions.

Amino Acid Substitutions in Aβ(1−40) Result in Varied Aggregation and Membrane Activity in the Presence of Lipid/PDA Biosensors. The Aβ(1−40) peptides all show increasing colorimetric response (Figure 3C) over time, demonstrating that each has a distinctive vesicle−peptide interaction event detected by the biosensor. Amino acid substitutions in Aβ(1−40) result in varied aggregation and membrane activity in the presence of lipid/PDA biosensors. All lipid/PDA vesicle systems (TBLE/PDA,

DOI: 10.1021/acsabm.9b00694
ACS Appl. Bio Mater. 2019, 2, 4966−4977

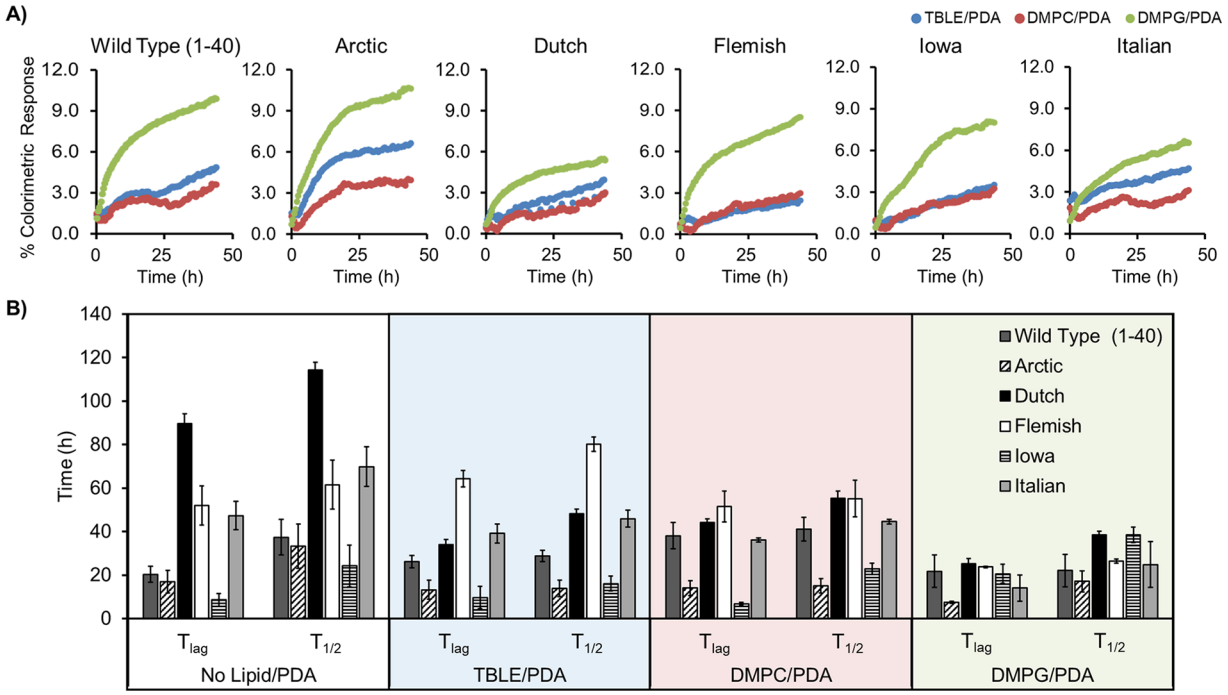

Figure 4. Aggregation of Wild Type Aβ(1−40) and Aβ (1−40) peptide variants display a variety of % CR and ThT fluorescence response in the presence of differing aggregation states and lipid/PDA environments. (A) Time-resolved % CR values of lipid/PDA vesicles composed of TBLE/PDA (blue line), DMPC/PDA (red line), and DMPG/PDA (green line) upon exposure to Wild Type, Arctic, Iowa, Italian, Dutch, and Flemish Aβ(1−40) are shown. % CR displays varying levels of response in correlation with aggregation state membrane activity. (B) ThT analysis of Aβ(1−40) peptide aggregation in the absence of lipid/PDA biosensors and in the presence of TBLE/PDA, DMPC/PDA, and DMPG/PDA biosensors. ThT fluorescence kinetic curves are modeled with a nonlinear (sigmoidal) least-squares regression and an estimated onset (lag time, T_{lag}) and time at half completion of the aggregation process ($T_{1/2}$) are obtained for each peptide−vesicle interaction. With the addition of vesicular biosensors composed of TBLE/PDA (blue), DMPC/PDA (red), and DMPG/PDA (green), and those with no biosensor present, distinct changes in the aggregation kinetics are reported in the presence of a lipid vesicle environment.

DMPC/PDA, and DMPG/PDA) exhibited a distinct change in % CR when exposed to prolonged amyloid peptide aggregation over a period of 44 h. This suggests that the lipid/PDA vesicle environment has the capability to identify vesicle−peptide interactions and structurally influence aggregation. In the time-resolved % CR studies of all Aβ(1−40) variants, the vesicle−peptide interactions show an initial response, followed by a gradual increase over time as peptides aggregate and transition from monomers to fibrils (Figure 4A). This trend is observed in all three lipid systems studied, indicating that they are appropriate model biosensor membranes to measure peptide−lipid interactions. Our data shows that the % CR is more pronounced in the DMPG/PDA vesicles, as compared to TBLE/PDA and DMPC/PDA vesicles.

To better analyze the relationship between fibrillization (measured by Thioflavin T (ThT) fluorescence) with membrane activity (measured by % CR), we compared time-resolved % CR curves with modeled ThT aggregation curves of the six Aβ(1−40) peptides incubated with no surface and also exposed to each lipid/PDA biosensor composition (Figure 4B). To understand which peptide aggregation state may trigger the interaction with certain lipid/PDA biosensors, we characterized the lipid/PDA responsive peptides by ThT. We use ThT, a selective, fluorescent benzathiole dye, whose fluorescence emission and sensitivity are enhanced upon binding to β-sheet-rich amyloid fibrils.[45] ThT assays were conducted in this study to characterize Aβ(1−40) peptide polymerization over time and determine membrane-active components of Aβ(1−40) peptide aggregation with lipid/PDA vesicles.

To measure the aggregation propensity of each Aβ(1−40) peptide variant, all peptides were measured at ∼20 μM by exposing solutions to ThT in the absence of lipid/PDA vesicles and in the presence of each lipid/PDA vesicle (TBLE/PDA, DMPC/PDA, or DMPG/PDA). Enhanced ThT fluorescence is indicative of protofibril and fibril aggregate formation. Analysis of ThT fluorescence under these conditions produces representative sigmoidal curves (normalized) of aggregation state (polymerization) kinetics for Wild Type Aβ(1−40) and Aβ(1−40) variant peptides (Figures S4 and S5). Fitting the kinetic data obtained from ThT assays with a sigmoidal model[40] enabled average T_{lag} (lag time) and $T_{1/2}$ (time at half completion of the aggregation process) to be obtained from kinetic curves of each Aβ(1−40) peptide (Figure 4B). Additionally, we used *ex situ* atomic force microscopy (AFM) to characterize aggregation state(s) morphology of Aβ(1−40) peptides (Figure S6). AFM images demonstrate that aggregation state is influenced by Aβ(1−40) peptide form (Wild Type or mutation) in coordination with subsequent reports.[11,43] The combination of ThT aggregation assays and AFM analysis in free solution (no lipid/PDA vesicles present during incubation) provides a means to verify aggregate formation and establish initial aggregation kinetics for later comparison.

Each peptide demonstrated a distinctive lag and growth phase, which varied due to the presence of the Aβ(1−40) point mutation and lipid/PDA biosensor (Figure 4B). All Aβ

DOI: 10.1021/acsabm.9b00694
ACS Appl. Bio Mater. 2019, 2, 4966−4977

peptides in the study reach a saturated aggregation state resulting in fibril formation by 160 h. The presence of ThT in the peptide solution did not affect the aggregation kinetics (at the concentrations used).[22] All Aβ(1−40) peptides show distinct fibril formation kinetics as measured by ThT fluorescence vs time, highlighting the extent to which mutation alters conversion to fibrils as described previously.[11,29−35,37,43] For the first 10 h of aggregation, all peptides are predominantly in a distinct lag phase for all three lipid/PDA biosensors. After ∼10 h, aggregation begins, and elongation (fibrillar growth) varies for each Aβ(1−40) peptide in the presence of a lipid environment. In comparison with T_{lag} and $T_{1/2}$ values obtained in the absence of lipid/PDA biosensors, aggregation kinetics are shown to be highly influenced by the presence of a model membrane surface. The presence of a lipid environment is seen to significantly decrease the lag phase for the Aβ(1−40) peptides in our study. Correlating with our high % CR measured in the presence of DMPG/PDA vesicles, we also measure a faster aggregation onset (shorter T_{lag}), as compared to TBLE/PDA and DMPC/PDA. Typically the fastest to aggregate are the Iowa mutation (D23N) and Arctic mutation (E22G), with an average T_{lag} (over all ThT assays) of 11.359 ± 3.12 and 12.878 ± 1.98 h, respectively. Flemish and Dutch were the slowest to aggregate with an average T_{lag} (over all ThT assays) of 47.872 ± 8.58 and 48.216 ± 14.359 h, respectively. Overall, we see that ThT assays of Aβ(1−40) peptide aggregation in the presence of TBLE/PDA, DMPC/PDA, and DMPG/PDA are faster than those in the absence of a membrane surface. The rapid aggregation is attributed to an induction of aggregation via vesicle−peptide interactions.

The fluorescence and colorimetric transitions induced by Wild Type Aβ(1−40) and Aβ(1−40) variants arising from familial mutations indicate the presence of membrane-active aggregate species, which bind to lipid/PDA vesicles. Interestingly, % CR shows immediate response (within 2 h) while ThT fluorescence (in the presence of all lipid/PDA vesicles) measures a distinct lag phase (ca. 10 h) during this time as seen by estimated T_{lag} and $T_{1/2}$ histograms (Figure 4B). With lag time being the time at which fibrillar aggregation initiates, for % CR to occur beforehand provides insight into which states of aggregation are contributing to membrane activity. The no-lag feature of the % CR biosensor suggests that % CR precedes changes in ThT fluorescence. Knowing the aggregation states present at different exposure times for each Aβ(1−40) peptide are dependent and influenced by the peptide amino acid sequence, our data suggests that the lipid/PDA biosensors are able to detect initial membrane-active aggregation states (monomeric/oligomeric) (within 0−4 h), followed by increased detection of more fibrillar aggregates. Lipid/PDA biosensor % CR and ThT fluorescence is lower for initial Aβ(1−40) peptide interactions of monomers and oligomers (exposure time 0−4 h) and higher for later interactions of protofibrils and fibrils (exposure time of over 7 h) (Figure 4A). As % CR detection increases, it is likely to be strongly associated and enhanced with increased membrane activity due to aggregation state (i.e., oligomer and/or β-sheet fibril formation).

Lastly, we tested the ability of lipid/PDA biosensors to detect and differentiate membrane-active interactions of early aggregates (monomers and small oligomers) vs later aggregates (protofibrils and/or fibrils). To understand which aggregation states may be the principal membrane-active components of the Aβ(1−40) peptides studied, aggregates were incubated with lipid/PDA vesicles followed by characterization of aggregate species via % CR and ThT. Upon ultracentrifugation, we defined larger aggregates (protofibrils and/or fibrils) to be confined in the pellet, and monomers and small oligomers to be contained in the supernatant. ThT fluorescence data in the presence of lipid/PDA biosensors shows the largest emission and greatest abundance to be in the resuspended pellet (Figure S7). The higher values of ThT fluorescence are indicative of β-sheet-rich amyloid fibril formation and enhanced ThT binding. Using ThT fluorescence as an indication of fibrillar Aβ(1−40) conformation, we verified the presence of soluble Aβ(1−40) species in the supernatant via a Protein A280 assay.

In Figure 5, a measurable % CR was detected after incubation of all six Aβ(1−40) peptide supernatant fractions in all lipid/PDA biosensors. This membrane activity measured in the supernatant attributes to the presence of oligomeric precursor species after 44 h. In addition, after 44 h of aggregation, we also see membrane activity with the protofibril/fibril species. Knowing protein aggregation to be a complex and dynamic process, the presence of a heterogeneous mixture of intermediary aggregates (i.e., oligomers and protofibrils) is to be expected after 44 h of incubation. In all three lipid/PDA biosensors, we measured a higher % CR in the supernatant fraction for Dutch and Flemish, while Wild Type, Arctic, Iowa, and Italian measured a higher % CR for the pellet fraction (Figure 5). The higher % CR response may be attributed to the presence of lipid/PDA vesicles inducing additional vesicle−peptide interaction event(s) and/or insertions into the lipid/PDA vesicle by larger aggregates (protofibrils and fibrils). At 44 h, our data suggests the membrane-active aggregates of Wild Type, Arctic, Iowa, and Italian to be predominantly fibrillar (i.e., protofibrils and fibrils), and oligomeric for Dutch and Flemish. The membrane-active aggregates measured here correspond with our obtained enhanced % CR results (Figure 4A), ThT fluorescence (Figure S5), and *ex situ* AFM images (Figure S6) at later time points of aggregation.

DISCUSSION

The aggregation pathway for any given amyloid-forming protein can vary considerably, depending on the protein sequence and its folding environment. Here, we have investigated Wild Type Aβ(1−40) and a selection of Aβ(1−40) variant peptides originating from familial mutations, in an effort to detect surface interaction events modulated by membrane-active aggregate species via lipid/PDA biosensors. Wild Type Aβ(1−40), a 40 residue cleavage product of the β-amyloid precursor protein (β-APP), is known to form senile plaques (aggregates) that build up between neuronal cells in AD. In families with an autosomal form of AD (familial AD, FAD), specific molecular defects that cause the disease have been identified by point mutations in the gene encoding the β-APP.[36] These mutations, most commonly associated with FAD, occur within or directly flanking the Aβ region of β-APP and near the hydrophobic core of Aβ(1−40) (amino acid residues 16−21). The mutations studied include Arctic (E22G) mutation, Dutch (E22Q) mutation, Flemish (A21G) mutation, Iowa (D23N) mutation, and Italian (E22K) mutation. Aβ variant peptides have diverse aggregation properties, and consequently, their interaction with the neuronal lipid bilayer is affected.[11,43] Not surprisingly, each pathogenic mutation increases overall Aβ production and presents as a unique pathology, ranging from severe cerebral

DOI: 10.1021/acsabm.9b00694
ACS Appl. Bio Mater. 2019, 2, 4966−4977

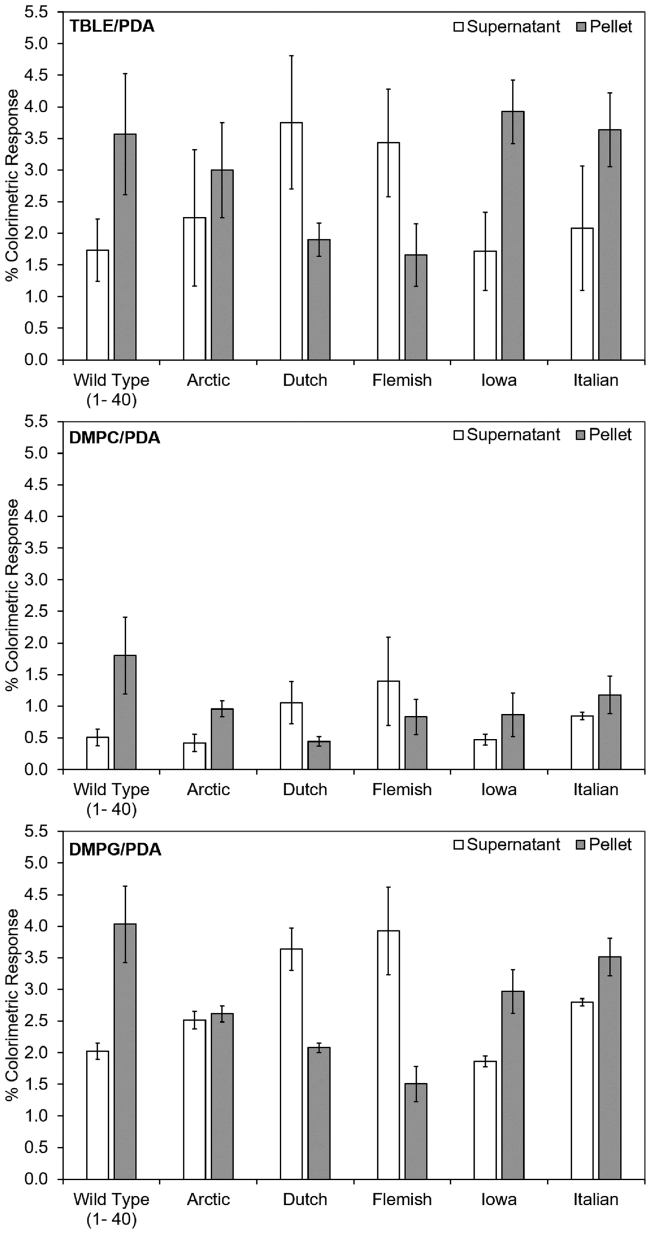

Figure 5. Quantification of lipid/PDA biosensor response with respect to distinct Aβ(1−40) peptide aggregate fractions. After 44 h of incubation, followed by ultracentrifugation, the average % CR values of Aβ(1−40) peptide smaller aggregates in the supernatant (i.e., soluble monomers and small oligomer aggregates) and larger aggregates in the pellet (i.e., protofibrils and fibrils) are shown for each lipid/PDA vesicle with standard error.

amyloid angiopathy (CAA) to AD-like plaque formation with varying ages of onset (Table S1).

Lipid membranes or bilayers are known to be the structural basis of biological and neuronal membranes. Knowing Aβ aggregation occurs on the neuronal cell surface, lipid/PDA biosensors are shown in our study to serve as model lipid membranes for detection. The presence of a lipid bilayer has been shown to modulate the Aβ(1−40) aggregate structure[46] despite differences in Aβ(1−40) preparation protocols[47] and to provide a distinctive environment to facilitate Aβ(1−40) peptide conformation into β-sheets.[48] Recent studies have identified that key interactions at surfaces modulate bilayer stability and affect Aβ(1−40) peptide sequence or point mutation aggregation in many ways (i.e., morphology, fibril formation, lipid interactions, etc.)[11−14,43,49,50] In this work, we demonstrate that changes in composition of lipid/PDA vesicles result in response differences due to diverse peptide−lipid interaction events. Model lipid membrane changes have significant influence on Aβ interactions, which may initiate amyloidogenic toxicity.[15] In particular, the lipid headgroup has been shown to be important in determining the membrane affinity of proteins.[22] The color changing mechanism measured via % CR is caused by the disruption of the lipid membrane interface by membrane-active aggregation states and possible insertion into the lipid layer. A greater lipid surface interaction(s) causes more pronounced perturbations of adjacent PDA domains and gives rise to an increase in % CR.[51] % CR thus serves as a means to directly detect aggregate interactions that occur exclusively at the lipid membrane surface. To explore this, the lipid/PDA biosensor examined interactions of membrane-active Aβ(1−40) peptide aggregates with model lipid membranes. With molecular interaction events affecting the biosensor surface, % CR measured is linked to the magnitude of vesicle−peptide interactions. We see that the increased colorimetric response is indicative of increased surface interaction events from the membrane-active aggregate species. All Aβ(1−40) peptide (Wild Type, Arctic, Dutch, Flemish, Iowa, and Italian) interaction is shown to be enriched (increased % CR over time of exposure) by the presence of an anionic, phospholipid membrane (DMPG/PDA), followed by TBLE/PDA (neutral lipid) and DMPC/PDA (zwitterionic, neutral), respectively. These observed interactions may be limited to the selected lipid systems and mutant peptides and could be further influenced by altering the lipid:peptide ratio and/or lipid composition. However, our findings correspond with studies indicating that Aβ(1−40) has been found to interact strongly with anionic, negatively charged membranes[52−54] and offer support to a proposed mechanism for initiating Aβ aggregation via electrostatic attraction between Aβ and lipid head groups.[55] This biosensor provides an advantageous detection method and quantitative assessment of sensitivity associated with membrane-active Aβ(1−40) peptide aggregation interacting with specific lipid membrane compositions in real time.

Using ThT fluorescence in conjunction with lipid/PDA biosensor % CR, we obtained insight into the probable Aβ(1−40) membrane-active peptide aggregation state(s) present. Amyloid formation is commonly known as a nucleation-dependent reaction with an initial lag phase where early monomers proliferate and grow via primary nucleation, followed be an elongation (growth) phase, and a final plateau/leveling off region.[56] Exposure of lipid/PDA biosensors to freshly prepared solutions of Aβ(1−40) peptides (Wild Type, Arctic, Dutch, Flemish, Iowa, and Italian) resulted in a distinct colorimetric and ThT response induced by changes in peptide−lipid interactions. One would expect the aggregation kinetics of the Aβ(1−40) peptides in this study to have a specific and detectable aggregation onset (T_{lag} ranging from 24 h to upward of 80 h) in free solution (free from surface effects). When in the presence of a lipid membrane environment, there is a discernible influence of membrane surface chemistries on the progression of peptide aggregate states into elongated, fibrillar structures. In the presence of all three lipid/PDA biosensors, we observed a more rapid T_{lag} in conjunction with an increased % CR in the initial lag phase as compared to the expected aggregation of the Wild Type

DOI: 10.1021/acsabm.9b00694
ACS Appl. Bio Mater. 2019, 2, 4966−4977

Aβ(1−40) and each Aβ(1−40) mutant. As % CR increases with additional membrane activity the presence of a lipid interface or membrane promotes aggregation. We detect that % CR supersedes ThT aggregation which demonstrates that lipid/PDA biosensors are able to detect initial stages of aggregation (i.e., interaction with monomer/oligomers) which are often undetected by typical ThT aggregation assays. One of the strengths of our analysis is that we can show sensitivity to monomeric/oligomeric species as well as protofibril/fibril aggregate species via lipid/PDA vesicles. From our studies, we can further elucidate how lipids may act to induce aggregation and provide enhancement of peptide aggregation in the presence of a lipid membrane. The ability to detect stages of membrane activity within the colorimetric, biometric, model membrane assay provides valuable insight into the role lipid surfaces play in modulating Aβ(1−40) aggregation with future impacts in understanding neurodegenerative onset.

Utilizing the biomimetic characteristics of lipid/PDA self-assembled vesicles, our studies provide understanding into the potential role lipid composition plays in dictating surface interaction of robust, membrane-active Aβ aggregates associated with FAD. Three familial point mutations we studied occur at the 22nd amino acid residue (Arctic (E22G), Dutch (E22Q), and Italian (E22K)) yet have drastically different lipid membrane surface interactions. Previous simulation studies suggested that mutations at the 22nd residue of Aβ retain a bend motif and are not linked to altered folding nucleation of Aβ, but rather to have long-range effects on parts of the full-length peptide.[57] AFM images also show that these three mutations form short fibrils overtime. Arctic was shown to be the most membrane-active of all peptides studied, followed by Italian and Dutch, respectively, for the 22nd residue. In all three mutations, a negative charge is removed. The electrostatic potential present at each lipid/PDA membrane surface is known to play a key role in increased Arctic−lipid interactions.[55] The Arctic mutation (E22G) replaces a polar, negative glutamate with a nonpolar, neutral glycine. As a result of the removal of the negative charge, the hydropathy index of the Arctic mutation increases drastically, making it more hydrophobic with increased stability. This amino acid substitution promotes the Arctic mutation to have the highest surface interaction events with all three lipid/PDA biosensors. The biomimetic biosensors used in this study effectively detected an increased membrane disturbing effect for the Arctic mutation that has been seen in both experimental and computational studies.[58] The Italian mutation (E22K) replaces a polar, negative glutamate with a polar, positive lysine. With the mutation inducing a change in charge, the lipid/PDA vesicle compositions are shown to promote increased electrostatic binding with lipid/PDA vesicles due to the Italian mutation becoming slightly more hydrophilic. The lipid−PDA interaction of Italian (E22K) is seen to be smaller than that of Arctic (E22G) for all lipid compositions due to less membrane activity of the aggregates. The Dutch mutation (E22Q) substitutes a polar, negative glutamate with a polar uncharged glutamine. Dutch remains a polar residue with measurable interaction, but to a much lesser extent than Italian (E22K) and Arctic (E22Q) due to the removal of charge (from negative to uncharged).

We then looked further at the familial mutations occurring at the 21st and 23rd amino acid residues. The Iowa mutation (D23N) replaces a polar, negative charged aspartic acid with a polar, neutral asparagine residue, with no change in hydrophobic character. On the 23rd residue, the removal of the negative charge appears to promote increased membrane activity and fibril formation. Simulations and studies reveal the Iowa mutation to affect peptide structure *in vitro* by forming a turn motif rather than a bend[57] and promoting fibrillogenesis.[33] The fast formation of fibrils and reduced ability of Iowa to be detected by lipid/PDA biosensors are related to the removal of a negative charge, and we suspect the turn motif. The Flemish mutation (A21G) replaces a nonpolar, neutral alanine with a nonpolar, neutral glycine. However, with this substitution, there is a large decrease in the protein's hydrophobic character which may attribute to the slow aggregation and fibril formation. During the first 30−40 h measured, Flemish (and Dutch) are typically in the oligomeric state (lag phase), having not begun to form β-sheet fibrillar structures. Interestingly, both oligomeric species have a high % CR (≥4%) and shorter T_{lag} and $T_{1/2}$ in the presence of DMPG/PDA. The high level of vesicle−peptide interaction with DMPG/PDA may be attributed to Aβ oligomers having a higher affinity for lipid membranes with a higher negative charge.[59] The proposed membrane-active aggregate species for Flemish and Dutch (at 44 h) are oligomers which corresponds to increased focus on implicating soluble oligomeric Aβ aggregates as the pathogenic molecular form in the amyloid cascade hypothesis.[60−64]

We are able to identify membrane-active amyloidogenic Aβ(1−40) aggregate states and detect their corresponding surface interactions via lipid/PDA biosensors. In this work, we confirm that vesicle−peptide Aβ(1−40) interaction events can be detected quickly and efficiently, as well as enhanced with variations in model lipid membrane chemistries. By utilizing lipid/PDA vesicles as a valid, practical, and reliable biosensor we have simplified and significantly decreased the amount of time to measure such interactions in comparison to conventional studies using AFM, nuclear magnetic resonance, microbiology, complex studies with immunotherapy, and magnetic resonance imaging.[11,43,65−69] Future work will involve expansion and development of the lipid/PDA biosensor library to encompass lipid environments closely associated with protein-misfolding and neurodegenerative diseases. Overall, the results presented here demonstrate that lipid/PDA biosensors can be used for detection and screening of membrane-active Aβ(1−40) aggregation to provide new details into how lipid membrane composition plays a distinct role in FAD.

CONCLUSION

We have used a biosensing, colorimetric, vesicle-binding assay as an innovative approach to promptly detect the presence of peptide−lipid interactions in membrane-active aggregate states of neurodegenerative FAD. Lipid/PDA biosensors provided comprehensive, time-resolved information about the appearance of vesicle−Aβ peptide interaction with various lipid surface chemistries. Direct measurements of vesicle−peptide interaction events using lipid/PDA assays reveal that mutant forms of Aβ(1−40) peptides have diverse and key surface interactions depending on the surface chemistry, mutation, and aggregation state present. This work provided insight into the role surfaces play in modulating vesicle−amyloidogenic peptide interactions, as well as providing new sensor knowledge of the lipid/PDA biosensor material. By understanding how protein aggregation and interaction can be affected by changes in lipid composition, lipid/PDA biosensors

DOI: 10.1021/acsabm.9b00694
ACS Appl. Bio Mater. 2019, 2, 4966−4977

have the potential to become a useful technique in future studies associated with amyloidogenic mechanisms of self-assembly with lipid membranes. We believe the use of these vesicle-binding biosensors will lead to earlier and advanced detection of amyloidogenic aggregation events which can ultimately lead to future improvement of therapies for AD and other neurodegenerative diseases.

■ ASSOCIATED CONTENT

Supporting Information

The Supporting Information is available free of charge on the ACS Publications website at DOI: 10.1021/acsabm.9b00694.

Schematics, statistical comparison, characterization of Aβ(1−40) peptide aggregation kinetics, AFM, lipid−PDA biosensor interactions, and Aβ(1−40) peptide characteristics (PDF)

■ AUTHOR INFORMATION

Corresponding Author

*E-mail: eyates@usna.edu.

ORCID

Elizabeth A. Yates: 0000-0002-7141-306X

Present Address

§M.P.D.: Morehouse School of Medicine, 720 Westview Drive SW, Atlanta, GA 30310, USA

Author Contributions

E.A.Y. conceived and designed the project. E.A.Y. performed lipid/PDA colorimetric response assays and ThT assays, prepped incubations, performed AFM, analyzed AFM images, and designed and completed ultracentrifugation studies. M.P.D. prepped, performed, and analyzed the lipid/PDA colorimetric response assay experiments. B.M.N. performed all statistical analysis on the data. Data analysis, writing, and editing were completed by E.A.Y. B.M.N. and M.P.D. participated in manuscript preparation. E.A.Y. directed the overall project. All authors approved the final version of the manuscript.

Notes

The authors declare no competing financial interest.

■ ACKNOWLEDGMENTS

This research was financially supported by the USNA Chemistry Department and the USNA Research Office Midshipman Research Support (MRS) Grant. The Naval Academy Research Council provided summer support [ONR Junior NARC to E.A.Y. (N0001416WX01475) and ONR Junior NARC to B.M.N. (N0001416WX01193)]. This work was also supported by the Defense Threat Reduction Agency Service Academy Research Initiative [MIPR HDTRA1620511 and HDTRA1723968 to E.A.Y.]. We are grateful to Dr. Leighanne Basta, Dr. Joan Shifflett, and Ms. Elizabeth Ward for helpful discussions and careful critiques of this manuscript.

■ ABBREVIATIONS

Aβ, β-amyloid; AD, Alzheimer's disease; AFM, atomic force microscopy; β-APP, β-amyloid precursor protein; BSA, bovine serum albumin; CAA, cerebral amyloid angiopathy; DMPC, 1,2-dimyristoyl-*sn*-glycero-3-phosphocholine; DMPG, 1,2-dimyristoyl-*sn*-glycero-3-phospho-(1′-rac-glycerol); DMSO, dimethyl sulfoxide; FAD, familial AD; HFIP, hexafluoroisopropanol; LUV, large, unilamellar vesicle; % CR, percent colorimetric response; PDA, polydiacetylene; TBLE, total brain lipid extract; ThT, Thioflavin T; TRCDA, 10,12-tricosadiynoic acid; TBS, Tris-buffered saline; NaOH, sodium hydroxide

■ REFERENCES

(1) Dobson, C. M. Protein Folding and Misfolding. *Nature* **2003**, *426*, 884−890.

(2) Anfinsen, C. B. Principles That Govern the Folding of Protein Chains. *Science* **1973**, *181* (4096), 223−230.

(3) Sunde, M.; Blake, C. C. From the Globular to the Fibrous State: Protein Structure and Structural Conversion in Amyloid Formation. *Q. Rev. Biophys.* **1998**, *31* (1), 1−39.

(4) Chiti, F.; Dobson, C. M. Protein Misfolding, Functional Amyloid, and Human Disease. *Annu. Rev. Biochem.* **2006**, *75*, 333−366.

(5) Chiti, F.; Dobson, C. M. Protein Misfolding, Amyloid Formation, and Human Disease: A Summary of Progress Over the Last Decade. *Annu. Rev. Biochem.* **2017**, *86*, 27−68.

(6) Kelly, J. W. The Alternative Conformations of Amyloidogenic Proteins and Their Multi-Step Assembly Pathways. *Curr. Opin. Struct. Biol.* **1998**, *8* (1), 101−106.

(7) Rambaran, R. N.; Serpell, L. C. Amyloid Fibrils: Abnormal Protein Assembly. *Prion* **2008**, *2* (3), 112−117.

(8) Barnes, D. E.; Yaffe, K. The Projected Impact of Risk Factor Reduction on Alzheimer's Disease Prevalence. *Lancet Neurol.* **2011**, *10* (9), 819−828.

(9) Gray, J. J. The Interaction of Proteins with Solid Surfaces. *Curr. Opin. Struct. Biol.* **2004**, *14* (1), 110−115.

(10) Simakova, O.; Arispe, N. J. The Cell-Selective Neurotoxicity of the Alzheimer's Aβ Peptide Is Determined by Surface Phosphatidylserine and Cytosolic ATP Levels. Membrane Binding Is Required for Aβ Toxicity. *J. Neurosci.* **2007**, *27* (50), 13719−13729.

(11) Pifer, P. M.; Yates, E. A.; Legleiter, J. Point Mutations in Aβ Result in the Formation of Distinct Polymorphic Aggregates in the Presence of Lipid Bilayers. *PLoS One* **2011**, *6* (1), 11.

(12) Burke, K. A.; Yates, E. A.; Legleiter, J. Amyloid-Forming Proteins Alter the Local Mechanical Properties of Lipid Membranes. *Biochemistry* **2013**, *52* (5), 808−817.

(13) Burke, K. A.; Yates, E. A.; Legleiter, J. Biophysical Insights into How Surfaces, Including Lipid Membranes, Modulate Protein Aggregation Related to Neurodegeneration. *Front. Neurol.* **2013**, *4*, 17.

(14) Moores, B.; Drolle, E.; Attwood, S. J.; Simons, J.; Leonenko, Z. Effect of Surfaces on Amyloid Fibril Formation. *PLoS One* **2011**, *6* (10), No. e25954.

(15) Drolle, E.; Negoda, A.; Hammond, K.; Pavlov, E.; Leonenko, Z. Changes in Lipid Membranes May Trigger Amyloid Toxicity in Alzheimer's Disease. *PLoS One* **2017**, *12* (8), No. e0182194.

(16) Zheng, F.; Wu, Z.; Chen, Y. A Quantitative Method for the Measurement of Membrane Affinity by Polydiacetylene-Based Colorimetric Assay. *Anal. Biochem.* **2012**, *420* (2), 171−176.

(17) Kolusheva, S.; Shahal, T.; Jelinek, R. Peptide−Membrane Interactions Studied by a New Phospholipid/Polydiacetylene Colorimetric Vesicle Assay. *Biochemistry* **2000**, *39* (51), 15851−15859.

(18) Kolusheva, S.; Wachtel, E.; Jelinek, R. Biomimetic Lipid/Polymer Colorimetric Membranes Molecular and Cooperative Properties. *J. Lipid Res.* **2003**, *44* (1), 65−71.

(19) Reppy, M. A.; Pindzola, B. A. Biosensing with Polydiacetylene Materials: Structures, Optical Properties and Applications. *Chem. Commun.* **2007**, *0* (42), 4317−4338.

(20) Jelinek, R.; Kolusheva, S. Polymerized Lipid Vesicles as Colorimetric Biosensors for Biotechnological Applications. *Biotechnol. Adv.* **2001**, *19* (2), 109−118.

(21) Cho, E.; Jung, S. Biomolecule-Functionalized Smart Polydiacetylene for Biomedical and Environmental Sensing. *Molecules* **2018**, *23* (1), 107.

DOI: 10.1021/acsabm.9b00694
ACS Appl. Bio Mater. 2019, 2, 4966−4977

(22) Sokolovski, M.; Sheynis, T.; Kolusheva, S.; Jelinek, R. Membrane Interactions and Lipid Binding of Casein Oligomers and Early Aggregates. *Biochim. Biophys. Acta, Biomembr.* **2008**, *1778* (10), 2341−2349.
(23) Jelinek, R.; Kolusheva, S. Biomolecular Sensing with Colorimetric Vesicles. In *Creative Chemical Sensor Systems*; Schrader, T., Ed.; Springer Berlin Heidelberg: Berlin, Heidelberg, 2007; Vol. *277*, pp 155−180.
(24) Stine, W. B.; Dahlgren, K. N.; Krafft, G. A.; LaDu, M. J. In Vitro Characterization of Conditions for Amyloid-β Peptide Oligomerization and Fibrillogenesis. *J. Biol. Chem.* **2003**, *278* (13), 11612−11622.
(25) Charych, D. H.; Nagy, J. O.; Spevak, W.; Bednarski, M. D. Direct Colorimetric Detection of a Receptor-Ligand Interaction by a Polymerized Bilayer Assembly. *Science* **1993**, *261* (5121), 585−588.
(26) Yates, E. A.; Owens, S. L.; Lynch, M. F.; Cucco, E. M.; Umbaugh, C. S.; Legleiter, J. Specific Domains of Aβ Facilitate Aggregation on and Association with Lipid Bilayers. *J. Mol. Biol.* **2013**, *425* (11), 1915−1933.
(27) Pires, A. C. d. S.; Soares, N. de F. F.; da Silva, L. H. M.; da Silva, M. d. C. H.; De Almeida, M. V.; Le Hyaric, M.; Andrade, N. J. de; Soares, R. F.; Mageste, A. B.; Reis, S. G. A Colorimetric Biosensor for the Detection of Foodborne Bacteria. *Sens. Actuators, B* **2011**, *153* (1), 17−23.
(28) Villalobos, P.; Chávez, M. I.; Olguín, Y.; Sánchez, E.; Valdés, E.; Galindo, R.; Young, M. E. The Application of Polymerized Lipid Vesicles as Colorimetric Biosensors for Real-Time Detection of Pathogens in Drinking Water. *Electron. J. Biotechnol.* **2012**, *15* (1), 3−4.
(29) Nilsberth, C.; Westlind-Danielsson, A.; Eckman, C. B.; Condron, M. M.; Axelman, K.; Forsell, C.; Stenh, C.; Luthman, J.; Teplow, D. B.; Younkin, S. G.; Näslund, J.; Lannfelt, L. The "Arctic" APP Mutation (E693G) Causes Alzheimer's Disease by Enhanced Aβ Protofibril Formation. *Nat. Neurosci.* **2001**, *4* (9), 887−893.
(30) Murakami, K.; Irie, K.; Morimoto, A.; Ohigashi, H.; Shindo, M.; Nagao, M.; Shimizu, T.; Shirasawa, T. Synthesis, Aggregation, Neurotoxicity, and Secondary Structure of Various Aβ1−42 Mutants of Familial Alzheimer's Disease at Positions 21−23. *Biochem. Biophys. Res. Commun.* **2002**, *294* (1), 5−10.
(31) De Jonghe, C.; Zehr, C.; Yager, D.; Prada, C.-M.; Younkin, S.; Hendriks, L.; Van Broeckhoven, C.; Eckman, C. B. Flemish and Dutch Mutations in Amyloid β Precursor Protein Have Different Effects on Amyloid β Secretion. *Neurobiol. Dis.* **1998**, *5* (4), 281−286.
(32) Nilsberth, C.; Westlind-Danielsson, A.; Eckman, C. B.; Forsell, C.; Axelman, K.; Luthman, J.; Younkin, S. G.; Näslund, J. The Arctic APP Mutation (E693G) Causes Alzheimer's Disease through a Novel Mechanism: Increased Amyloid Bprotfibril Formation and Decreased Amyloid Blevels in Plasma and Conditioned Media. *Neurobiol. Aging* **2000**, *21*, 58.
(33) Van Nostrand, W. E.; Melchor, J. P.; Cho, H. S.; Greenberg, S. M.; Rebeck, G. W. Pathogenic Effects of D23N Iowa Mutant Amyloid β-Protein. *J. Biol. Chem.* **2001**, *276* (35), 32860−32866.
(34) Watson, D. J.; Selkoe, D. J.; Teplow, D. B. Effects of the Amyloid Precursor Protein Glu693→Gln 'Dutch' Mutation on the Production and Stability of Amyloid β-Protein. *Biochem. J.* **1999**, *340* (3), 703−709.
(35) Levy, E.; Carman, M. D.; Fernandez-Madrid, I. J.; Power, M. D.; Lieberburg, I.; van Duinen, S.; Bots, G. T.; Luyendijk, W.; Frangione, B. Mutation of the Alzheimer's Disease Amyloid Gene in Hereditary Cerebral Hemorrhage, Dutch Type. *Science* **1990**, *248* (4959), 1124−1126.
(36) Citron, M.; Oltersdorf, T.; Haass, C.; McConlogue, L.; Hung, A. Y.; Seubert, P.; Vigo-Pelfrey, C.; Lieberburg, I.; Selkoe, D. J. Mutation of the β-Amyloid Precursor Protein in Familial Alzheimer's Disease Increases β-Protein Production. *Nature* **1992**, *360* (6405), 672−674.
(37) Hatami, A.; Monjazeb, S.; Milton, S.; Glabe, C. G. Familial Alzheimer's Disease Mutations within the Amyloid Precursor Protein Alter the Aggregation and Conformation of the Amyloid-β Peptide. *J. Biol. Chem.* **2017**, *292* (8), 3172−3185.
(38) Kyte, J.; Doolittle, R. F. A Simple Method for Displaying the Hydropathic Character of a Protein. *J. Mol. Biol.* **1982**, *157* (1), 105−132.
(39) Fawzi, N. L.; Kohlstedt, K. L.; Okabe, Y.; Head-Gordon, T. Protofibril Assemblies of the Arctic, Dutch, and Flemish Mutants of the Alzheimer's Aβ1−40 Peptide. *Biophys. J.* **2008**, *94* (6), 2007−2016.
(40) Hellstrand, E.; Boland, B.; Walsh, D. M.; Linse, S. Amyloid β-Protein Aggregation Produces Highly Reproducible Kinetic Data and Occurs by a Two-Phase Process. *ACS Chem. Neurosci.* **2010**, *1* (1), 13−18.
(41) Nečas, D.; Klapetek, P. Gwyddion: An Open-Source Software for SPM Data Analysis. *Cent. Eur. J. Phys.* **2012**, *10* (1), 181−188.
(42) Lebègue, E.; Farre, C.; Jose, C.; Saulnier, J.; Lagarde, F.; Chevalier, Y.; Chaix, C.; Jaffrezic-Renault, N. Responsive Polydiacetylene Vesicles for Biosensing Microorganisms. *Sensors* **2018**, *18* (2), 599.
(43) Yates, E. A.; Cucco, E. M.; Legleiter, J. Point Mutations in Aβ Induce Polymorphic Aggregates at Liquid/Solid Interfaces. *ACS Chem. Neurosci.* **2011**, *2* (6), 294−307.
(44) Kwakowsky, A.; Potapov, K.; Kim, S.; Peppercorn, K.; Tate, W. P.; Ábrahám, I. M. Treatment of Beta Amyloid 1−42 (Aβ_{1-42})-Induced Basal Forebrain Cholinergic Damage by a Non-Classical Estrogen Signaling Activator *in Vivo*. *Sci. Rep.* **2016**, *6*, 21101.
(45) Biancalana, M.; Koide, S. Molecular Mechanism of Thioflavin-T Binding to Amyloid Fibrils. *Biochim. Biophys. Acta, Proteins Proteomics* **2010**, *1804* (7), 1405−1412.
(46) Accardo, A.; Shalabaeva, V.; Cotte, M.; Burghammer, M.; Krahne, R.; Riekel, C.; Dante, S. Amyloid β Peptide Conformational Changes in the Presence of a Lipid Membrane System. *Langmuir* **2014**, *30* (11), 3191−3198.
(47) Yates, E. A.; Legleiter, J. Preparation Protocols of Aβ(1−40) Promote the Formation of Polymorphic Aggregates and Altered Interactions with Lipid Bilayers. *Biochemistry* **2014**, *53* (45), 7038−7050.
(48) Khondker, A.; Alsop, R. J.; Rheinstädter, M. C. Membrane-Accelerated Amyloid-β Aggregation and Formation of Cross-β Sheets. *Membranes* **2017**, *7* (3), 49.
(49) Sharp, J. S.; Forrest, J. A.; Jones, R. A. L. Surface Denaturation and Amyloid Fibril Formation of Insulin at Model Lipid−Water Interfaces. *Biochemistry* **2002**, *41* (52), 15810−15819.
(50) Kowalewski, T.; Holtzman, D. M. In Situ Atomic Force Microscopy Study of Alzheimer's β-Amyloid Peptide on Different Substrates: New Insights into Mechanism of β-Sheet Formation. *Proc. Natl. Acad. Sci. U. S. A.* **1999**, *96* (7), 3688−3693.
(51) Jelinek, R.; Kolusheva, S. Membrane Interactions of Host-Defense Peptides Studied in Model Systems. *Curr. Protein Pept. Sci.* **2005**, *6* (1), 103−114.
(52) Maltseva, E.; Brezesinski, G. Adsorption of Amyloid β (1−40) Peptide to Phosphatidylethanolamine Monolayers. *ChemPhysChem* **2004**, *5* (8), 1185−1190.
(53) Thakur, G.; Micic, M.; Leblanc, R. M. Surface Chemistry of Alzheimer's Disease: A Langmuir Monolayer Approach. *Colloids Surf., B* **2009**, *74* (2), 436−456.
(54) Ding, H.; Schauerte, J. A.; Steel, D. G.; Gafni, A. β-Amyloid (1−40) Peptide Interactions with Supported Phospholipid Membranes: A Single-Molecule Study. *Biophys. J.* **2012**, *103* (7), 1500−1509.
(55) Bokvist, M.; Lindström, F.; Watts, A.; Gröbner, G. Two Types of Alzheimer's β-Amyloid (1−40) Peptide Membrane Interactions: Aggregation Preventing Transmembrane Anchoring Versus Accelerated Surface Fibril Formation. *J. Mol. Biol.* **2004**, *335* (4), 1039−1049.
(56) Arosio, P.; Knowles, T. P. J.; Linse, S. On the Lag Phase in Amyloid Fibril Formation. *Phys. Chem. Chem. Phys.* **2015**, *17* (12), 7606−7618.
(57) Krone, M. G.; Baumketner, A.; Bernstein, S. L.; Wyttenbach, T.; Lazo, N. D.; Teplow, D. B.; Bowers, M. T.; Shea, J.-E. Effects of

DOI: 10.1021/acsabm.9b00694
ACS Appl. Bio Mater. 2019, 2, 4966−4977

Familial Mutations on the Folding Nucleation of the Alzheimer Amyloid β-Protein. *J. Mol. Biol.* **2008**, *381* (1), 221−228.
(58) Poojari, C.; Strodel, B. Stability of Transmembrane Amyloid β-Peptide and Membrane Integrity Tested by Molecular Modeling of Site-Specific Aβ42 Mutations. *PLoS One* **2013**, *8* (11), No. e78399.
(59) Wong, P. T.; Schauerte, J. A.; Wisser, K. C.; Ding, H.; Lee, E. L.; Steel, D. G.; Gafni, A. Amyloid-β Membrane Binding and Permeabilization Are Distinct Processes Influenced Separately by Membrane Charge and Fluidity. *J. Mol. Biol.* **2009**, *386* (1), 81−96.
(60) Broersen, K.; Rousseau, F.; Schymkowitz, J. The Culprit behind Amyloid β Peptide Related Neurotoxicity in Alzheimer's Disease: Oligomer Size or Conformation? *Alzheimer's Res. Ther.* **2010**, *2* (4), 12.
(61) Hardy, J.; Selkoe, D. J. The Amyloid Hypothesis of Alzheimer's Disease: Progress and Problems on the Road to Therapeutics. *Science* **2002**, *297* (5580), 353−356.
(62) Korczyn, A. D. The Amyloid Cascade Hypothesis. *Alzheimer's Dementia* **2008**, *4* (3), 176−178.
(63) Goure, W. F.; Krafft, G. A.; Jerecic, J.; Hefti, F. Targeting the Proper Amyloid-β Neuronal Toxins: A Path Forward for Alzheimer's Disease Immunotherapeutics. *Alzheimer's Res. Ther.* **2014**, *6* (4), 42.
(64) Reiss, A. B.; Arain, H. A.; Stecker, M. M.; Siegart, N. M.; Kasselman, L. J. Amyloid Toxicity in Alzheimer's Disease. *Rev. Neurosci.* **2018**, *29* (6), 613−627.
(65) Schenk, D.; Hagen, M.; Seubert, P. Current Progress in Beta-Amyloid Immunotherapy. *Curr. Opin. Immunol.* **2004**, *16* (5), 599−606.
(66) Baltes, C.; Princz-Kranz, F.; Rudin, M.; Mueggler, T. Detecting Amyloid-β Plaques in Alzheimer's Disease. In *Magnetic Resonance Neuroimaging: Methods and Protocols*; Modo, M., Bulte, J. W. M., Eds.; Methods in Molecular Biology; Humana Press: Totowa, NJ, 2011; pp 511−533.
(67) Funke, S. A. Detection of Soluble Amyloid-β Oligomers and Insoluble High-Molecular-Weight Particles in CSF: Development of Methods with Potential for Diagnosis and Therapy Monitoring of Alzheimer's Disease. *Int. J. Alzheimer's Dis.* **2011**, *2011*, 1.
(68) Tycko, R. Molecular Structure of Aggregated Amyloid-β: Insights from Solid-State Nuclear Magnetic Resonance. *Cold Spring Harbor Perspect. Med.* **2016**, *6* (8), a024083.
(69) Petkova, A. T.; Ishii, Y.; Balbach, J. J.; Antzutkin, O. N.; Leapman, R. D.; Delaglio, F.; Tycko, R. A Structural Model for Alzheimer's β-Amyloid Fibrils Based on Experimental Constraints from Solid State NMR. *Proc. Natl. Acad. Sci. U. S. A.* **2002**, *99* (26), 16742−16747.

DOI: 10.1021/acsabm.9b00694
ACS Appl. Bio Mater. 2019, 2, 4966−4977